



Available online at www.sciencedirect.com

ScienceDirect

Journal of Nutritional Biochemistry

Journal of Nutritional Biochemistry 112 (2023) 109174

RESEARCH PAPER

Role of liquid fructose/sucrose in regulating the hepatic transcriptome in a high-fat Western diet model of NAFLD

Yuwen Luo^{a,†}, Lauren N. Woodie^{a,1,†}, Emily C. Graff^{b,c}, Jian Zhang^a, Savanah Fowler^a, Xiaozhu Wang^b, Xu Wang^{b,d}, Ann Marie O'Neill^a, Michael W. Greene^{a,c,*}

^a Department of Nutritional Sciences

^b Department of Pathobiology

^c Boshell Metabolic Diseases and Diabetes Program, Auburn University, Auburn, Alabama, USA

^d HudsonAlpha Institute for Biotechnology, Huntsville, Alabama, USA

Received 8 March 2022; received in revised form 8 August 2022; accepted 19 August 2022

Abstract

Nonalcoholic fatty liver disease (NAFLD), which ranges from simple steatosis to nonalcoholic steatohepatitis (NASH), is the most common chronic liver disease. Yet, the molecular mechanisms for the progression of steatosis to NASH remain largely undiscovered. Thus, there is a need for identifying specific gene and pathway changes that drive the progression of NAFLD. This study uses high-fat Western diet (HFWD) together with liquid sugar [fructose and sucrose (F/S)] feeding for 12 weeks in mice to induce obesity and examine hepatic transcriptomic changes that occur in NAFLD progression. The combination of a HFWD+F/S in the drinking water exacerbated HFWD-induced obesity, hyperinsulinemia, hyperglycemia, hepatic steatosis, inflammation, and human and murine fibrosis gene set enrichment that is consistent with progression to NASH. RNAseq analysis revealed differentially expressed genes (DEGs) associated with HFWD and HFWD+F/S dietary treatments compared to Chow-fed mice. However, liquid sugar consumption resulted in a unique set of hepatic DEGs in HFWD+F/S-fed mice, which were enriched in the complement and coagulation cascades using network and biological analysis. Cluster analysis identified Orosomucoid (ORM) as a HFWD+F/S upregulated complement and coagulation cascades gene that was also upregulated in hepatocytes treated with TNF α or free fatty acids in combination with hypoxia. ORM expression was found to correlate with NAFLD parameters in obese mice. Taken together, this study examined key genes, biological processes, and pathway changes in the liver of HFWD+F/S mice in an effort to provide insight into the molecular basis for which the addition of liquid sugar promotes the progression of NAFLD.

© 2022 Elsevier Inc. All rights reserved.

Keywords: NAFLD; Liver; High-fat diet; Liquid sugar; Transcriptome; ORM.

1. Introduction

Nonalcoholic fatty liver disease (NAFLD) has become the most common chronic liver disease in both children and adults [1], paralleling the increased prevalence of obesity and diabetes during the last decades [2]. The NAFLD spectrum ranges from simple steatosis (fatty liver) to nonalcoholic steatohepatitis (NASH), which can lead to more serious clinical conditions of cirrhosis and liver can-

cer (hepatocarcinoma). NAFLD is a multiple system disease and a clinical manifestation of the metabolic syndrome [3]. Indeed, it has been proposed that metabolic (dysfunction) associated fatty liver disease "MAFLD" is a more appropriate term than NAFLD to more accurately reflect the pathogenesis and help with patient stratification [4,5]. However, despite this new understanding of NAFLD, current treatment options for NAFLD are limited largely due to the lack of adequate animal models for diet-induced NAFLD [6]. In addition, the molecular mechanisms for the progression of steatosis to NASH remain largely undiscovered. Thus, there exists a need for characterizing animal models of diet-induced NAFLD to identify specific genes and gene pathways that drive the progression of NAFLD to aid in the development of new therapeutic targets.

This study uses a high-fat Western diet together with liquid fructose/sucrose-fed mice to investigate transcriptomic changes involved in the development and progression of chronic liver disease. In order to mimic the consumption of sugar in adults [7] and chil-

^{*} Corresponding author at: Michael W. Greene, Ph.D., Director, AU Metabolic Phenotyping Laboratory, Department of Nutritional Sciences, 260 Lem Morrison Dr., 101C PSB, Auburn University, Auburn, AL, 36849, USA.

E-mail address: mwgreene@auburn.edu (M.W. Greene).

[†] Co first authors.

¹ Current Address: Institute for Diabetes, Obesity and Metabolism, Department of Endocrinology and Metabolism, Perelman School of Medicine, University of Pennsylvania, Philadelphia, PA 19104, USA.

dren [8], obesity-linked overnutrition models have been developed based on added sugar in the form of fructose and/or sucrose. Fructose, a highly lipogenic sugar, is thought to contribute to the development and the severity of NAFLD [9] though both indirect and direct fructose metabolism pathways [10-12]. The high-fat Western diet with liquid fructose/sucrose consumption mouse model of obesity was originally developed as a model of NAFLD progression [13-15], and has been reported to model obese humans with mild NASH [16]. However, an in-depth analysis comparing the transcriptomic changes in the livers of this model to those differentially regulated in human NAFLD and NASH has, to our knowledge, yet to be reported. Our group has recently examined the metabolic phenotype of high-fat Western diet (HFWD)-fed mice with liquid fructose/sucrose in the drinking water and confirmed that this approach represents a good physiologic and metabolic model to investigate the mechanism underlying the progression of NAFLD [17].

To examine genes and gene pathways that drive the progression of NAFLD, we used RNA sequencing (RNAseq), a comprehensive, sensitive, quantitative, and unbiased approach which measures the RNA expression profile more accurately over a greater dynamic range than microarray-based technologies [18] that have previously been used to examine the expression of genes in NAFLD progression in animal models [19,20] and humans [21,22]. Using RNAseq, we were able to provide a global view of the unique transcriptomic changes induced by the addition of fructose/sucrose drinking water to a HFWD. Here, we report the exacerbation of gross NAFLD parameters in the livers of mice consuming sugary drinking water on top of a HFWD along with the key biological processes, pathways, and genes involved in accelerated progression. Furthermore, through gene set enrichment analysis (GSEA) our findings suggest that this animal model is a representation of the molecular human NAFLD/NASH condition.

2. Methods and materials

2.1. Animals

Male C57BL/6N mice from Harlan Laboratories (Somerville, NI) were housed one per cage in the Auburn University Veterinary Research Building, an AAALAC accredited animal facility, in 12:12-h light-dark, temperature at 22°C, and humiditycontrolled rooms. Mice were provided with standard laboratory chow and water ad libitum in accordance with an Institutional Animal Care and Use Committee approved protocol for 1-week to allow for acclimatization to the animal facility. No procedures were undertaken that caused more than minimal pain, distress, or discomfort. After the 1-week acclimation period, mice (n = 8, 7-week old) remained on the standard Chow diet (Teklad Global Rodent Diet 2018; energy density 3.1 kcal/g) or received a high-fat Western diet (HFWD) (Test Diets, Cat. #5TJN; energy density 4.49 kcal/g) containing ~12% and 40% energy from fat, respectively, with or without sugar (42 g/L) added to the drinking water at a ratio of 55% fructose/45% sucrose (F/S). The amount and composition of sugar added to the drinking water was based on the work of Tetri et al. who developed a NAFLD animal model in which a HFWD was combined with a high fructose corn syrup equivalent in the drinking water [15]. The composition of fat in the diets was 30% from lard, 30% from butterfat, and 30% from Crisco. The sample size estimate was based on our prior NAFLD study with HFWD and HFWD+F/S-fed mice [17]. After 12 weeks on their respective diets, mice were fasted for 5 h (including changing the F/S drinking water to tap water in the HFWD+F/S-fed mice) and then euthanized by inhalation of CO2. Blood immediately drawn from the caudal vena cava and blood glucose was sampled using an Accu-Check blood glucometer. After clotting at room temperature, the sample was centrifuged at 12,000 g for 15 min at 4°C. The serum was removed and stored frozen at -80°C until tested. Liver and eWAT were excised and weighed. Tissue samples were fixed in 10% buffered formalin prior to paraffin embedding and flash frozen (liver) or immersed in RNAlater (Life Techonologies, Carlsbad, CA) (eWAT) and stored at -80°C until used for RNA extraction.

For the Orosomucoid (ORM) expression validation study and NAFLD correlation analysis, RNA extracted from the livers and NAFLD parameter data from male C57BL/6NHsd mice fed a low fat Western diet (LFWD) (Test Diets, Cat #5TJS) or a high-fat Western diet (HFWD) (Test Diets, Cat #5TJN) with or without sugar (42 g/L) added to the drinking water at a ratio of 55% fructose/45% sucrose was obtained from a previously described cohort [17].

2.2. Liver tissue histological and lipid analysis

Paraffin-embedded sections were stained with hematoxylin and eosin examined in a blinded fashion by a board-certified veterinary pathologist. NAFLD was scored using a general scoring system for rodent models, which is based on the human NAS (NAFLD activity score) grading criteria [23]. Briefly, micro- and macro-vesicular steatosis were separately scored and the severity was graded, based on the percentage of the total area affected, into the following categories: 0 (<5%), 1 (5-33%), 2 (34-66%), and 3 (>66%). The level of hepatocellular hypertrophy, defined as cellular enlargement more than 1.5 times the normal hepatocyte diameter, was scored, based on the percentage of the total area affected, into the following categories: 0 (<5%), 1 (5-33%), 2 (34-66%), and 3 (>66%). Hepatic inflammation was analyzed by counting the number of inflammatory foci per field at ×100 magnification (view size 3.1 mm²) in five different fields per specimen. NAFLD score was calculated for each liver biopsy based on the sum of scores for steatosis, hypertrophy and inflammation. TGs were assayed using a kit from Thermo Scientific (Rockford, IL) and normalized to the protein content measured using the BCA protein assay reagent (Thermo Scientific/Pierce, Rockford, IL).

2.3. In-vitro experiments

AML12 (alpha mouse liver 12) cells were purchased from the American Type Culture Collection and cultured in DMEM medium (Life Technologies, Grand Island, NY) supplemented with 10% fetal bovine serum (FBS) (Atlanta Biologicals, Flowery Branch, GA) and 1% penicillin-streptomycin solution (Cellgro, Manassas, VA). Cells were maintained at 37°C in a 5% CO2 atmosphere. Cells were treated with tumor necrosis factor-alpha (TNF α) or free fatty acids (FFAs) in combination with hypoxia. TNF α and FFA have been widely used to induce insulin resistance in cultured cells [24–28], while hypoxia treatment has been shown to induce insulin resistance in adipocytes [29] and hepatocytes [30]. AML12 cells were serum deprived, treated with TNF α (10, 20, 50, and 100 ng/mL) or with the saturated FFA palmitate (0.4 and 0.9 mM) with or without hypoxia (1% O₂) treatment for 16 hours, and then stimulated with insulin for 2 min. Cell lysates were analyzed by immunoblotting.

2.4. RNA-seq library preparation and sequencing

We randomly selected four mice from chow, five mice from HFWD, and HFWD+F/S respectively, to isolate total RNA from liver tissue for RNAseq analysis. We confirmed that the mice selected were representative of their dietary group for whole body, epididymal adipose, and liver weights. RNeasy Plus Universal Kits (Qiagen, Valencia, CA) was used to isolate total RNA from frozen liver following the manufacturer's protocol. All RNA-seq library procedures were performed at the Genomic Services Laboratory (GSL), HudsonAlpha Institute for Biotechnology. Initial QC quantification of the extracted total RNA was done by using Qubit Fluorometer (Invitrogen), and the quality of the extracted RNA was evaluated using an Agilent 2,100 Bioanalyzer (Agilent Technologies, Santa Clara, CA).

Five hundred ng of total RNA was taken for proceeding to downstream RNA-seq applications. First, ribosomal RNA (rRNA) was removed using Ribo-Zero Gold (Yeast) kit (Epicenter, Madison, WI) using manufacturer's recommended protocol. Immediately after the rRNA removal the RNA was fragmented and primed for the first strand synthesis using the NEBnext First Strand synthesis module (New England BioLabs Inc., Ipswich, MA). The second strand synthesis was then performed using the NEBnext Second Strand synthesis module. Following this the samples were taken into standard library preparation protocol using NEBNext DNA Library Prep Master Mix Set for Illumina with slight modifications. Briefly, end-repair was done followed by A-tailing and custom adapter ligation. Post-ligated materials were individually barcoded with unique in-house Genomics Service Laboratory (GSL) primers and amplified through 12 cycles of PCR. Library quantity was assessed by Qubit 2.0 Fluorometer, and the library quality was estimated by utilizing a DNA 1,000 chip on an Agilent 2.100 Bioanalyzer, Accurate quantification of the final libraries for sequencing applications was determined using the qPCR-based KAPA Biosystems Library Quantification kit (Kapa Biosystems, Inc., Woburn, MA). Each library was diluted to a final concentration of 12.5 nM and pooled equimolar prior to clustering. Paired-End (PE) sequencing (50 million per sample, 100bp) was on an Illumina HiSeq2500 sequencer (Illumina, Inc.).

2.5. Processing of RNA-seq reads

Approximately 50 million, 100bp, PE reads were generated from each sample. Quality control checks on raw sequence data from each sample was performed using FastQC (Babraham Bioinformatics, London, UK). Raw reads were mapped to the reference mouse genome mm9 using TopHat v2.0 [31,32] with two mismatches allowed and other default parameters. The alignment metrics of the mapped reads were estimated using SAMtools [33]. Aligned reads were then imported onto the commercial data analysis platform, Avadis NGS (Strand Scientifics, CA, USA). After quality inspection, the aligned reads were filtered on the basis of read quality metrics where reads with a base quality score less than 30, alignment score less than 95, and mapping quality less than 40 were removed. The remaining reads were

then filtered on the basis of their read statistics, where missing mates, translocated, unaligned, and flipped reads were removed. The reads list was then filtered to remove duplicates. Samples were grouped and quantification of transcript abundance was done on this final read list using Trimmed Means of M-values (TMM) [34] as the normalization method. Differential expression of genes were calculated on the basis of fold change (using default cut-off $\geq \pm 2.0$) observed between dietary treatments, and the *P-value* of the differentially expressed gene list was estimated by *z-score* calculations using determined by Benjamini Hochberg FDR correction of .05 [35]. Spearman correlation was used to test count correlation of different replicates within each treatment group. One chow sample with low correlation was excluded from the subsequent analysis (data not shown). Volcano plots, used to illustrate upand downregulated gene expression events, were generated for each diet comparison. Venn diagrams were created to identify differentially expressed genes between each diet comparison. The data set (GSE89296) is available at NCBI Gene Expression Omnibus database (www.ncbi.nlm.nih.gov/geo).

2.6. Biological and network analysis

Biological processes and pathway analysis were performed using Database for Annotation, Visualization, and Integrated Discovery (DAVID; version 6.8; david.ncifcrf.gov) [36,37] with the full list of hepatic genes expressed in the chow-, HFWD-, and HFWD+F/S-fed mice used as the background. Gene Ontology was performed in DAVID to identify biological processes (GOTERM_BP_ALL). Gene enrichment analyses were performed using Kyoto Encyclopedia of Genes and Genomes (KEGG) [38] to identify the most significantly affected unique canonical pathways. The top 10 biological processes and top five KEGG pathways were filtered for functionally related terms (very high, high, and moderate) to identify overlapping terms.

To construct a protein-protein interaction (PPI) network from the DEGs, the Search Tool for the Retrieval of Interacting Genes (STRING; version 10.0; string-db.org) online database for PPI network construction [39] was used in Cytoscape (version 3.5.1) [40], a bioinformatics platform for visualizing molecular interaction networks. To identify the top three clusters (highly interconnected regions) in the networks, the Cytoscape plugin app "Molecular Complex Detection" (MCODE; version 1.5.1) [41] was run using the following parameters: MCODE score, >4; degree cutoff, 10; node score cutoff, 0.2; and k-score, 2. The top three clusters were identified by MCODE Score (density of the cluster multiplied by the number of members). Gene enrichment analyses from the cluster DEGs were performed in DAVID using KEGG to identify the most significantly affected unique canonical pathways.

2.7. Gene set enrichment analysis (GSEA)

GSEA was performed using 1,000 permutations and the phenotype permutation type with the desktop GSEA program (version 4.1.0) [42]. Annotations of human ensemble gene ID to the Molecular Signature Database (MSigDB) v7.0 were performed. Enrichment plots were presented to visualize the data. Normalized enrichment score (NES) which accounts for gene set size differences and gene sets and the expression dataset correlations was reported. Nominal *P*-values were reported for analyses performed using individual gene sets. A nominal *P*-value of less than .05 was considered statistically significant. The false discovery rate (FDR) q-value, which is the estimated probability that the NES represents a false positive finding, were reported in analyses performed with more than one gene set. An FDR q-value of less than 0.10 was considered statistically significant which is lower than 0.25 which is recommended in the GSEA User Guide [43].

To analyze gene set enrichment in hepatic transcriptomic data from HFWD+F/S-fed mice, the following gene sets were used: (1) a set of 232 upregulated hepatic genes from high-fat diet fed LDL-receptor knockout mice identified as molecular fibrosis signature based on correlation with 8 differentially upregulated proteins [44]; (2) a set of 20 genes highly correlated to hepatic fibrosis in high-fat diet fed LDL-receptor knockout mice that were derived from the 232 gene molecular fibrosis signature [44]; (3) a set of 90 hepatic genes significantly differentially regulated in human samples from NASH patients compared to control liver tissue [45]; and (4) a set of 38 genes differentially regulated between the lobular inflammation and advanced fibrosis histological human samples [46].

Gene set enrichment in 2 independent human NASH cohorts was performed using the following upregulated and downregulated gene sets derived from the pathways identified in the gene clusters from the HFWD+F/S networks: (1)Cluster 1 - Steroid Biosynthesis, Complement & Coagulation Cascades, and Biosynthesis of Antibiotics; (2) Cluster 2 – Ribosome; and (3) Cluster 3 - Complement & Coagulation Cascades. The human cohort liver transcriptomic data was obtained from the Gene Expression Omnibus (GEO) database, using the "GEOquery" Bioconductor package [47].

2.8. Human NASH cohorts used for GSEA

The Universitätsklinikum Dresden cohort (German) analyzed patients who exhibited all the stages of NAFLD [48]. The transcriptome data, GSE48452, had 73 patients including control (n=14), healthy obese (n=27), steatosis (n=14), and NASH (n=18). We performed a comparison of "Control versus NASH." The Duke University cohort (Duke) analyzed 72 patients classified as obese or overweight, exhibiting

NAFLD with varying fibrosis stages [49]. The transcriptome data, GSE49541, had 72 patients including mild NAFLD with fibrosis stage 0-1 (n=40) and advanced NAFLD with fibrosis stage 3-4 (n=32). We performed a comparison of "Mild versus Advanced." Both the German and Duke cohorts lacked patient dietary assessments.

2.9. RT-PCR analysis

RNeasy Plus Universal Kits (Qiagen, Valencia, CA) was used to isolate total RNA from frozen liver and AML12 cells following the manufacturer's protocol. RNA quantity and quality were assessed using a ThermoScientific NanoDrop OneC (Thermo Fisher, Waltham, MA). Reverse transcription was performed using the RT² First Strand Kit (Qiagen, Valencia, CA). qPCR was performed with RT² SYBR Green qPCR Mastermix (Qiagen, Valencia, CA) and gene-specific primers (SABiosciences, Fredrick, MD) using MyiQ Real-Time PCR systems (Bio-Rad, Hercules, CA). After amplification, melt curve analysis was performed to confirm the specificity of the reaction. All measurements were performed in triplicate. GAPDH was used as a reference gene to normalize gene expression. The $2^{\wedge - \Delta\Delta CT}$ method was used to analyze the qPCR data and measure relative expression differences [50].

3. Statistical analyses

Statistical analysis was performed using GraphPad Prism 6 (La Jolla, CA). The results are presented as means \pm SEs. Statistical significance of gene expression data was analyzed by Student's t-test (α =0.05) using the chow group as a control. Statistical significance between groups was determined by one-way analysis of variance (α =0.05) followed by Newman-Keuls test (α =0.05). Linear regression was performed to compare gene expression results [log₂(fold-change)] obtained by RNA-seq and qPCR.

4. Results

4.1. Fructose/sucrose drinking water exacerbates markers of metabolic disease in HFWD-fed male mice

Male C57Bl/6N mice aged 7 weeks were placed on a Chow or HFWD with or without 42 g/L F/S in the drinking water for 12 weeks. The Chow group served as the control group. After 12 weeks, mice fed the HFWD gained more weight than Chow, however, this was exacerbated by the addition of sugary drinking water with the HFWD+F/S gaining 44% and 12% more body weight than the Chow and HFWD groups, respectively (*P*<.05, Table 1). Liver weight was also markedly higher in the HFWD+F/S group (48% vs. control, and 19% vs. HFWD, Table 1). eWAT weight as a percent of body weight was significantly higher in both HFWD-fed group compared to the Chow group (*P*<.05, Table 1). Finally, fasting blood glucose levels were significantly elevated in the HFWD+F/S-fed mice compared to both Chow and HFWD (*P*<.05, Table 1).

Body and organ weights, and blood glucose level in mice.

	Chow	HFWD †	HFWD±F/S [†]
Body weight (g)	$30.9{\pm}1.3^{a}$	39.7 ± 1.2^{b}	44.6±0.8°
Liver weight (g)	1.26 ± 0.05^{a}	2.05 ± 0.22^{b}	2.72 ± 0.22^{c}
Liver/Body weight (%)	4.10 ± 0.10^{a}	5.09 ± 0.43^{ab}	6.06 ± 0.38^{b}
eWAT* (g)	1.14 ± 0.20^{a}	2.28 ± 0.12^{b}	2.46 ± 0.09^{b}
eWAT/Body weight (%)	3.57 ± 0.47^{a}	5.80 ± 0.35^{b}	5.54 ± 0.29^{b}
Glucose (mg/dL)	146.5 ± 13.5^{a}	163.7 ± 14.9^{a}	214.4 ± 10.6^{b}

Abbreviations: HFWD, high-fat Western diet; F/S, fructose/sucrose; eWAT, epididymal white adipose tissue.

* C57BI/6N mice aged 7 weeks were placed on a chow or HFWD with or without 42 g/L F/S in the drinking water for 12 weeks. The Chow group served as the control group. Values represents the means \pm SE; n=8. Data was analyzed by ANOVA and pairwise comparisons were made using Newman-Keuls test. Different letters indicate significantly different values at P<.05.

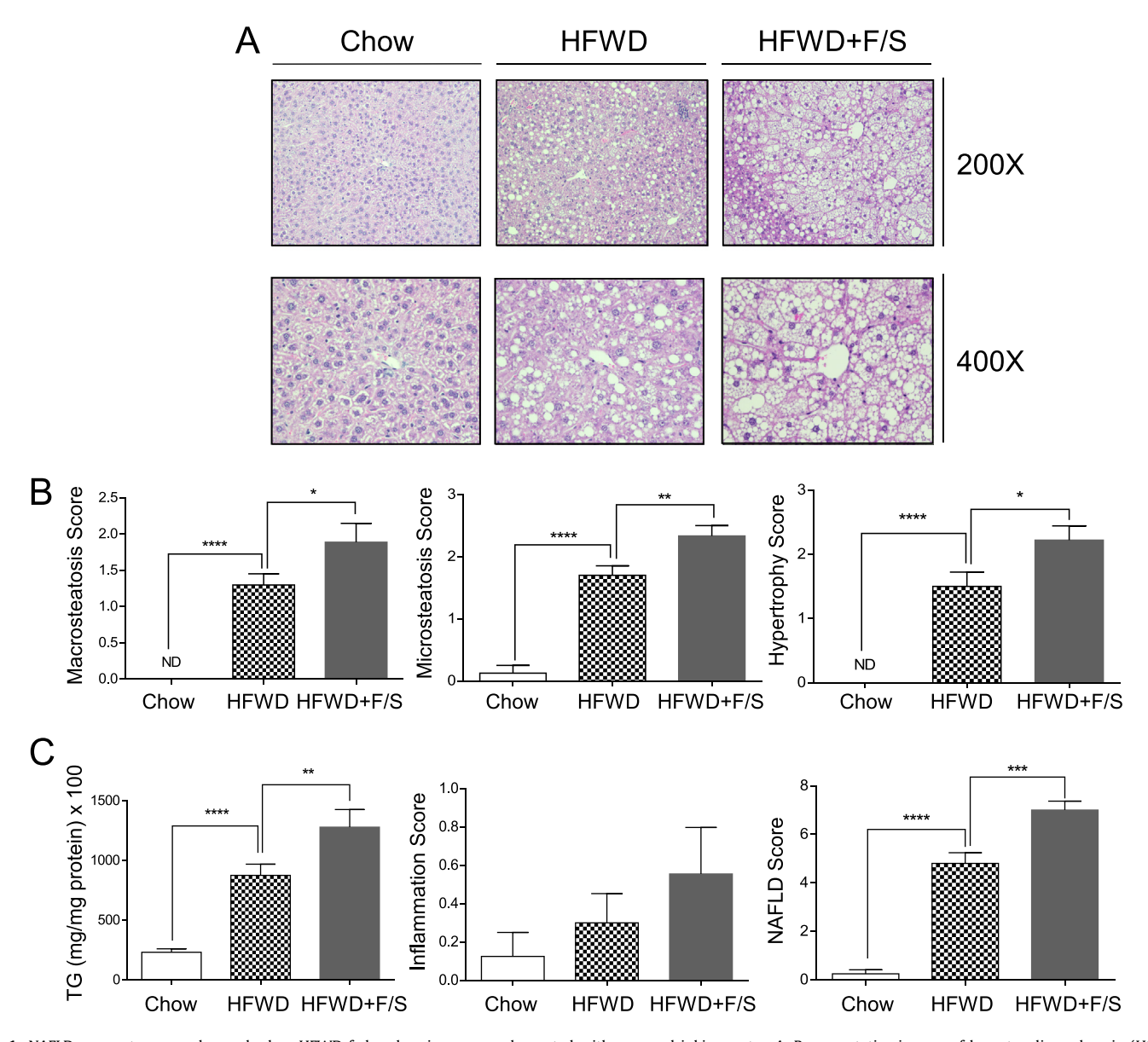


Fig. 1. NAFLD parameters are advanced when HFWD-fed male mice are supplemented with sugary drinking water. A. Representative images of hematoxylin and eosin (H&E)-stained liver sections. B–D. Macro- and microsteatosis and hypertrophy scoring of H&E-stained liver sections. E. Quantification of hepatic triglyceride content. F. NAFLD score calculated based on the sum of scores for micro-/macrosteatosis, hypertrophy and inflammation. Data are expressed as means \pm SE, n=8 per group. ND = not detected. * P < .05; *** P < .01; **** P < .001; ****

4.2. NAFLD parameters are advanced when HFWD-fed male mice are supplemented with fructose/sucrose drinking water

Given the stark exacerbation of sugary drinking water on the HFWD phenotype, we next investigated its impact on histologic markers of NAFLD and NASH (e.g., hepatic steatosis, hypertrophy, and inflammation [51]). Histological scoring of stained liver tissue sections from the diet treatment groups at 12-week revealed that both HFWD and HFWD+F/S-fed mice demonstrated substantial steatosis as indicated by greater macro- and micro-vesicular steatosis scores as well as hepatocellular hypertrophy compared with the control group (P<.05, Fig. 1A–D). However, the greatest steatosis (macrosteatosis and microsteatosis) and hypertrophy scores were observed in the HFWD+F/S group (Fig. 1B–D). Confirming the histological impression, liver TG levels at 12-week were significantly elevated in the HFWD+F/S group compared to both Chow and HFWD (P<.01, Fig. 1E). Steatosis, hypertrophy, and in-

flammation scores for each animal were summed to generate a NAFLD total score, which is a validated histological NAFLD scoring system in rodent [23]. As shown in Figure 1F, the HFWD+F/S group had a significantly greater NAFLD total score than both the Chow-(P<.001) and the HFWD-fed (P<.01) groups.

4.3. Supplementing HFWD-fed male mice with fructose/sucrose drinking water reprograms the hepatic transcriptome

Providing sugary drinking water to mice fed a HFWD significantly amplified the metabolic and histo-pathologic impacts of the unhealthy diet. Therefore, to gain an unbiased, global view of the HFWD+F/S on the hepatic transcriptome, we performed high-throughput sequencing of liver samples from each of the three dietary groups. We obtained approximately 150, 149, and 141 million high quality reads from the liver of Chow, HFWD, and HFWD+F/S-fed mice, respectively. Approximately 65%, 67%, and 74% of the

Table 2
Gene Ontology of the top ten most significant biological processes overlapping or uniquely regulated in livers from HFWD-fed and HFWD+F/S-fed mice.

Group	Pathway	Count [†]	Fold [‡]	P-value*
Overlap	Lipid metabolic process	100	4.0	5.83E-31
	Small molecule biosynthetic process	49	5.3	7.92E-18
	Fatty acid metabolic process	39	5.2	4.22E-13
	Lipid localization	31	4.4	5.57E-08
	Single-organism catabolic process	41	2.8	1.39E-05
	Cellular carbohydrate metabolic process	22	4.1	1.83E-04
	Response to extracellular stimulus	29	3.1	5.68E-04
	Regulation of biological quality	109	1.6	9.32E-04
	Anion transport	27	3.1	1.17E-03
	Sulfur compound metabolic process	22	3.7	1.26E-03
HFWD	Intestinal absorption	8	11.5	2.98E-04
	Phospholipid metabolic process	20	3.1	1.66E-03
	Reactive nitrogen species metabolic process	9	5.9	5.87E-03
	Thioester biosynthetic process	6	11.3	6.35E-03
	Dicarboxylic acid transport	8	6.8	6.52E-03
	Regulation of multicellular organismal process	84	1.5	7.89E-03
	Isoprenoid biosynthetic process	6	9.5	1.30E-02
	Localization	144	1.3	2.57E-02
	Blood circulation	21	2.3	2.62E-02
	Negative regulation of lipid catabolic process	5	10.7	3.06E-02
HFWD+F/S	Cellular amino acid catabolic process	15	6.9	2.69E-06
	Response to organic substance	145	1.5	1.67E-05
	Regulation of catalytic activity	90	1.7	1.05E-04
	Biosynthetic process	244	1.3	2.83E-04
	Regulation of wound healing	17	4.0	3.57E-04
	Carbohydrate biosynthetic process	20	3.4	4.36E-04
	Programmed cell death	95	1.6	5.56E-04
	Cellular response to nutrient levels	19	3.4	5.91E-04
	Negative regulation of response to stimulus	73	1.7	9.25E-04
	Regulation of molecular function	106	1.5	1.21E-03

^{*} Benjamini adjusted *P*-value.

RNAseq reads were uniquely mapped to annotated mouse genes in chow, HFWD, and HFWD+F/S group, respectively (Supplemental Table 1). DEGs identified by RNAseq were validated by with RT-qPCR by selecting 4 upregulated genes (Cidea, Myom3, Hr, and Spon), 2 genes with less than 0.5-log2 fold (Slc25 and Bmp2), and 3 downregulated genes (Mapk4, Nkrf, and Fnip1) (Supplementary Fig. 1). RT-qPCR results were significantly correlated with the RNAseq results by linear regression analysis (R²=0.910, P value = <.0001).

First, we confirmed using transcriptomics that HFWD+F/S-fed mice represent an advance form of NAFLD compared to HFWD-fed mice. We used 2 independent murine fibrosis gene sets to perform a gene set enrichment analysis (GSEA) comparing hepatic RNAseq data from HFWD+F/S-fed mice to the chow- and HFWD-fed mice (Supplementary Table 2). Both murine fibrosis gene sets with an FDR P<.01 were significantly enriched in livers from HFWD+F/S-fed mice (Supplementary Fig. 2).

We then identified differentially expressed genes (DEGs) in the livers of Chow, HFWD and HFWD+F/S-fed mice using EdgeR to count read depths per gene transcript and detected significant DEGs based on fold change (≥ 2) [52]. Volcano plots (Fig. 2A and B) were generated to illustrate up- and down-regulated gene for each comparison (HFWD vs Chow and HFWD+F/S vs. Chow, respectively). In total, 442 genes were differentially expressed (≥ 2 -fold) in the HFWD-fed compared to Chow-fed mice, of which 246 genes

were upregulated and 196 genes were downregulated (Fig. 2A and C). When sugary drinking water was added to the HFWD, 688 genes were differentially expressed, including 340 downregulated genes and 348 upregulated genes (Fig. 2B and C). Overall, 314 differentially expressed hepatic genes were identified as shared between the HFWD and HFWD+F/S groups (Fig. 2C).

Of particular interest, however, were the 128 and 374 uniquely regulated genes in the HFWD and HFWD+F/S groups, respectively (Fig. 2C). When analyzed for GO Biological Processes, we found that lipid metabolism pathways were significantly enriched in the overlapping gene set, validating the finding of increased lipid accumulation in both HFWD-fed livers when compared to Chow (Fig. 2D, left panel). When the 374 genes uniquely regulated by HFWD+F/S were analyzed for GO terms, we found enrichment for diverse biological processes such as cellular amino acid catabolic process, response to organic substance, and regulation of catalytic activity (Fig. 2D, right panel). We were specifically intrigued by the inflammation-related (regulation of wound healing) and apoptosis-related (programmed cell death) processes uniquely enriched in the HFWD+F/S-fed mice. Further gene set interrogation by KEGG pathway analysis produced consistent results. One of the top uniquely enriched KEGG pathways in the HFWD+F/S group was the complement and coagulation cascades pathway, which is heavily involved in the immune response to injury (Fig. 2E).

[†] number of genes in the pathway.

[‡] fold enrichment in the pathway.

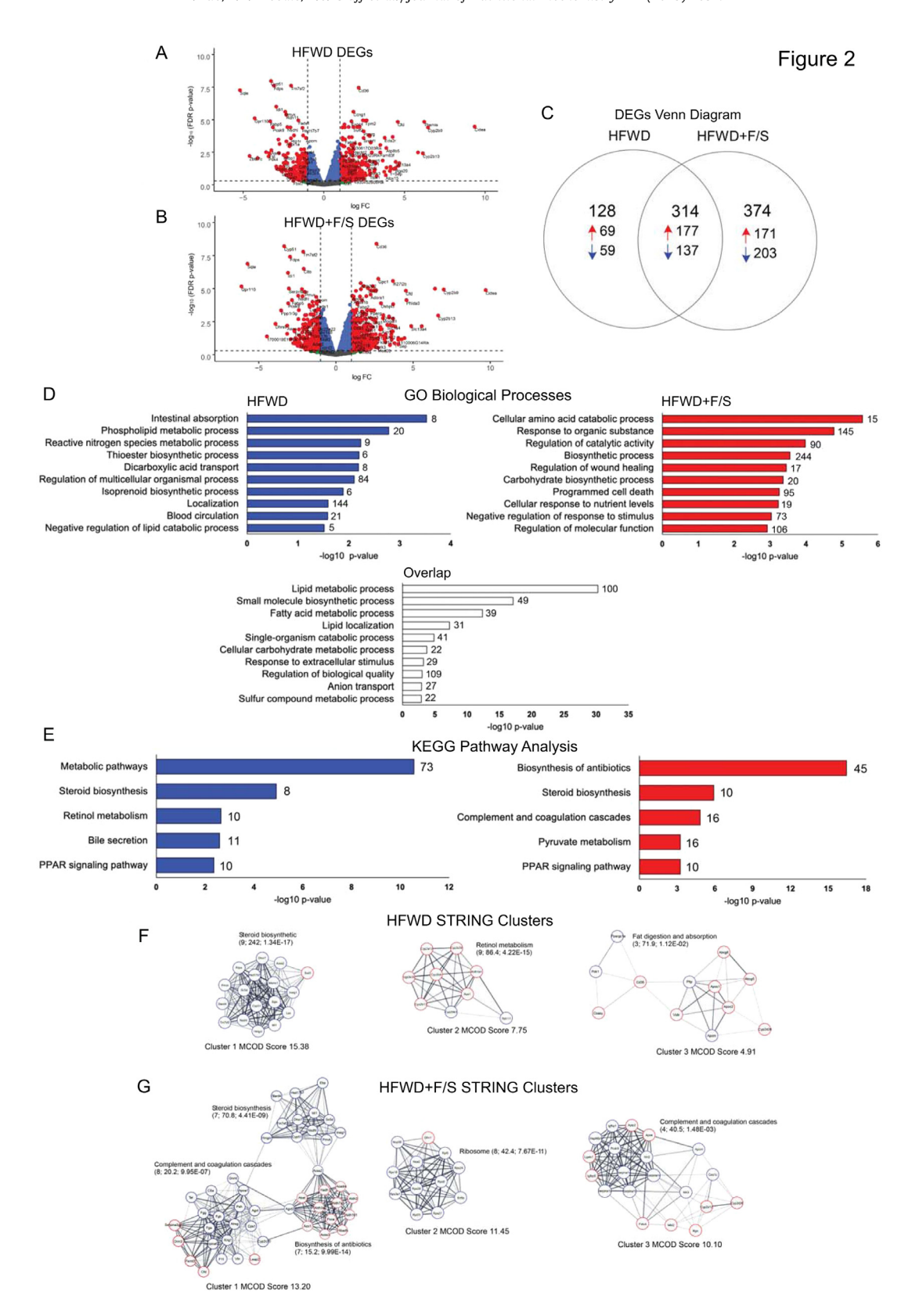


Fig. 2. Supplementing HFWD-fed male mice with sugary drinking water reprograms the hepatic transcriptome. A-B. Volcano plots illustrating differentially expressed genes (DEGs) between the HFWD vs Chow groups (A) and the HFWD+F/S vs Chow groups (B). C. Venn diagram illustrating the numbers of unique and overlapping DEGs between HFWD and HFWD+F/S. The number of DEGs that were downregulated are noted next to blue arrows and the number of upregulated DEGs are noted next to red arrows. D. Gene Ontology of the top ten most significant biological processes overlapping or uniquely regulated in livers from HFWD-fed and HFWD+F/S-fed mice. Bar length represents -log10 p-value for each pathway. Numbers at the end of each bar represents number of genes in the pathway found in our dataset. E. KEGG pathway analysis for the five most of genes in the pathway found in our dataset. F-G. DEGs were used to construct the top three STRING network clusters identified by the MCODE score for the HFWD (F) and HFWD+F/S groups (G). KEGG pathways enriched in the clusters were identified using DAVID. Shown for each KEGG pathway is the number of genes in the pathway and the FDR p-value. Upregulated genes are shown in red and downregulated genes are shown in blue.

Next, we performed network STRING cluster analysis on the HFWD and HFWD+F/S DEGs to identify specific genes and clusters of genes involved in the exacerbation of NAFLD observed after exposure to sugary drinking water. In the HFWD network, clusters enriched for steroid biosynthesis (P=1.34E-17), retinol metabolism (P=4.22E-15), and fat digestion and absorption (P=1.12E-02) were observed (Fig. 2F). In contrast, HFWD+F/S network clusters were enriched for complement and coagulation cascades in two separate clusters (P=9.95E-07 and 1.48E-03, respectively) and ribosome (P=7.67E-11) in a single cluster (Fig. 2G).

4.4. Genes for the orosomucoid (ORM) family of inflammatory proteins are uniquely overexpressed in the livers of HFWD+F/S-fed male mice

Pathway and network cluster analyses revealed the complement and coagulation cascades pathway as uniquely relevant in the livers of HFWD+F/S-fed mice. The HFWD+F/S complement and coagulation cascade network cluster identified the gene Orosomucoid 3 (ORM3) as significantly linked (Fig. 2G). Furthermore, ORM3 was upregulated 5-fold in the HFWD+F/S group compared to HFWD group (Fig. 3A, left panel). The Orosomucoid (ORM) (also called α -1 acid glycoprotein) gene product is an acute phase protein for which there is a family of 3 genes in mice (ORM1-3) and two genes in humans (ORM1-2) [53,54]. To validate our RNAseq data on the expression of ORM3, RT-qPCR was performed livers from the Chow, HFWD and HFWD+F/S-fed mice. Consistent with our RNAseq data, ORM3 expression was elevated approximately 5-fold in HFWD+F/S fed mice compared to HFWD fed mice (Fig. 3A, right panel). In addition, ORM2 but not ORM1 hepatic expression was also significantly elevated approximately 2-fold in HFWD+F/S fed mice compared to HFWD fed mice (data not shown).

To further validate ORM3 as a significant factor in sugary drinking water exacerbating HFWD-induced NAFLD, we examined hepatic expression of ORM1-3 in an independent cohort of mice. The HFWD and HFWD+F/S groups received similar treatment as in the present work, however, a low-fat Western diet was used for the control group in the independent work [17]. ORM3 expression was upregulated approximately 5-fold in HFWD+F/S-fed mice compared to HFWD fed mice (Fig. 3B, far right panel). ORM1 and ORM2 hepatic expression was significantly elevated to a similar level as ORM3 in HFWD+F/S fed mice compared to HFWD fed mice (Fig. 3C, left and middle panel). Correlation analysis of ORM1-3 gene expression and NAFLD parameters revealed a positive correlation of the ORMs with body weight, normalized liver weight, and serum alanine aminotransferase (ALT), a marker of liver dysfunction (Fig. 3C). Specifically, ORM3 was significantly positively correlated with body weight (P=.02) and normalized liver weight (P=.02) while ORM1 and ORM3 gene expression was significantly positively correlated with ALT (P<.05, Fig. 3C). A negative correlation was observed between ORM1-3 gene expression and fibrosis score; however, only ORM2 was significantly negatively correlated (P=.03, Fig. 3C).

4.5. An in vitro model of insulin resistant hepatocytes recapitulates overexpression of ORM in response to metabolic dysfunction

To examine whether *ORM* gene expression can be induced directly in hepatocytes, we developed cellular hepatocyte models of insulin resistance in AML12 cells. We sought to model insulin resistance which we have previously reported is exacerbated in HFWD+F/S-fed mice compared to HFWD-fed mice [17]. As shown in Supplementary Figure 3, AKT-Ser473 phosphorylation was significantly blunted in AML12 hepatocytes upon insulin stimulation in both TNF α and FFA treated cells incubated

in a hypoxic condition. The greatest inhibition of insulin stimulated AKT-Ser473 phosphorylation was observed in the FFA 0.9 mM + Hypoxia group. We next examined the expression of *ORM* genes in this model. Consistent with our findings *in vivo*, the expression of *ORM3* gene was significantly highly elevated (approximately 33-fold and 67-fold) in AML12 treated with FFA 0.9 mM + hypoxia and TNF α 100 ng/ml +hypoxia, respectively (Supplementary Fig. 3C). In addition, the combination of TNF α or FFA with hypoxia treatment induced gene expression of *ORM3* in a dose-dependent manner. Similar results were observed in the expression of *ORM1* and *ORM2* genes as well (Supplementary Fig. 3C).

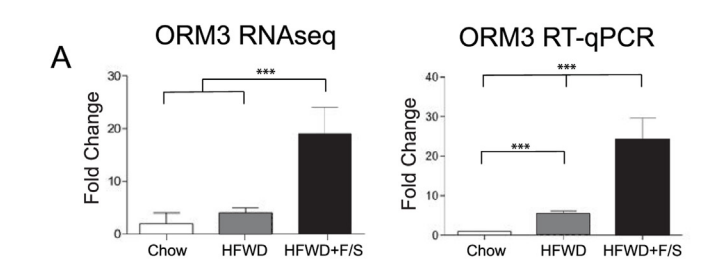
4.6. Gene set enrichment analysis (GSEA) validation of the HFWD+F/S-fed mouse as a model for human NAFLD

Our results to this point indicate the HFWD+F/S-fed male mouse as a murine model of advanced diet-induced NAFLD. However, to confirm the translation of our model to human NAFLD we performed GSEA with two independent human NASH cohorts (Supplementary Table 2) on RNAseq from HFWD+F/S and two additional independent human NASH cohorts on the cluster-identified gene sets from Figure 2F. For our HFWD+F/S RNAseq, the human NASH gene set (Normalized enrichment score 1.33, FDR q-value = 0.081) was significantly enriched in livers from HFWD+F/S-fed mice (Fig. 4A, left panel), while the fibrosis vs inflammation (Normalized enrichment score 1.29, FDR q-value = 0.138) gene set was enriched but did not reach our threshold for statistical significance (Fig. 4A, right panel).

To examine the relevance of the three hepatic HFWD+F/S network clusters, GSEA was performed using genes within each cluster and transcriptomic data from two independent human NASH cohorts from Germany and Duke [48,49]. We focused the analysis on the downregulated complement and coagulation cascades genes in clusters 1 and 3 and the ribosome genes in cluster 2 (Supplementary Table 3) because gene sets from these clusters contained at least 10 genes. In the German cohort in which Control vs. NASH was compared, we observed a trend that the gene set for downregulated genes in the complement and coagulation cascades for cluster 1 (Normalized enrichment score 1.36, FDR q-value = 0.107) and a significant enrichment for cluster 3 (Normalized enrichment score 1.51, FDR q-value = 0.075) were negatively correlated with NASH (Fig. 4B) which is consistent with the genes being downregulated in the hepatic HFWD+F/S network clusters. We also observed that the ribosome gene cluster (Normalized enrichment score 1.49, FDR q-value = 0.051) was negatively correlated with NASH in the German cohort which is consistent with the genes being downregulated in the hepatic HFWD+F/S network clusters (Fig. 4B). Next, gene set enrichment in the Duke cohort which compares mild to advanced NASH was assessed. We observed that the gene set for downregulated genes in the complement and coagulation cascades for cluster 1 (Normalized enrichment score 1.67, FDR q-value = 0.005) but not cluster 3 (Normalized enrichment score 0.98, FDR q-value = 0.796) was negatively correlated with advanced NASH (Fig. 4C). There was not a correlation with the ribosome gene set with advanced NASH (Fig. 4C).

5. Discussion

In this study we used RNAseq to provide an unbiased, global view of the unique changes induced in the hepatic transcriptome of male mice when fructose/sucrose drinking water is added to a HFWD. Using this technique, we were able to demonstrate the main DEGs, biological processes, and pathways involved in the progression of NAFLD. The relevance of the regulated transcriptome



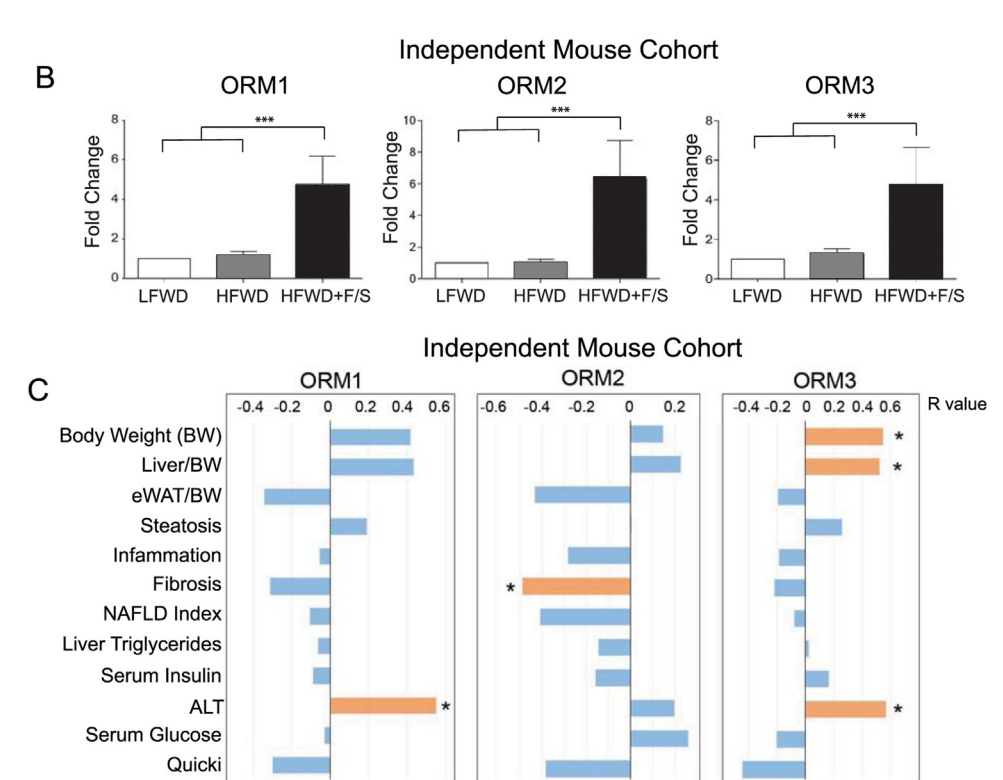


Fig. 3. Genes for the orosomucoid (ORM) family of inflammatory proteins are uniquely overexpressed in the livers of HFWD+F/S-fed male mice. A. Fold change in ORM3 gene expression assessed by RNAseq (left panel) and validated by RT-qPCR (right panel) in the livers of Chow-, HFWD- and HFWD+F/S-fed mice. B. RT-qPCR analysis of ORM1 (left panel), ORM2 (middle panel) and ORM3 (right panel) in the livers of mice from an independent study where they were fed either a LFWD, HFWD or HFWD+F/S for 12 wks. Data are expressed as means \pm SE, n=8 per group. ND = not detected. * P<.05; ** P<.01; ***. C. Spearman correlation analysis of published murine NAFLD parameters (Luo et al. 2015, 14) against ORM1-3 expression. Spearman correlation coefficients (R) are shown. Significant positive (R>1) and negative (R<1) correlations are shown using orange bars and denoted with a * (P<.05).

Table 3
Gene Ontology of the top 5 significant KEGG pathways in livers from HFWD- and HFWD+F/S-fed mice.

Group	Annotation	Pathway	Count [†]	Fold [‡]	P-value*
HFWD	KEGG	Metabolic pathways	73	2.4	2.74E-11
		Steroid biosynthesis	8	17.4	1.23E-05
	Bile secretion	10	5.8	2.57E-03	
		Retinol metabolism	11	5.1	2.24E-03
		PPAR signaling pathway	10	5.2	4.42E-03
HFWD+F/S KEGG	KEGG	Biosynthesis of antibiotics	45	5.1	3.52E-17
		Steroid biosynthesis	10	12.7	1.27E-06
		Complement and coagulation cascades	16	5.1	1.53E-05
		PPAR signaling pathway	16	6.2	5.62E-04
		Pyruvate metabolism	10	6.2	5.62E-04

^{*} Benjamini adjusted P-value.

[†] number of genes in the pathway.

[‡] fold enrichment in the pathway.

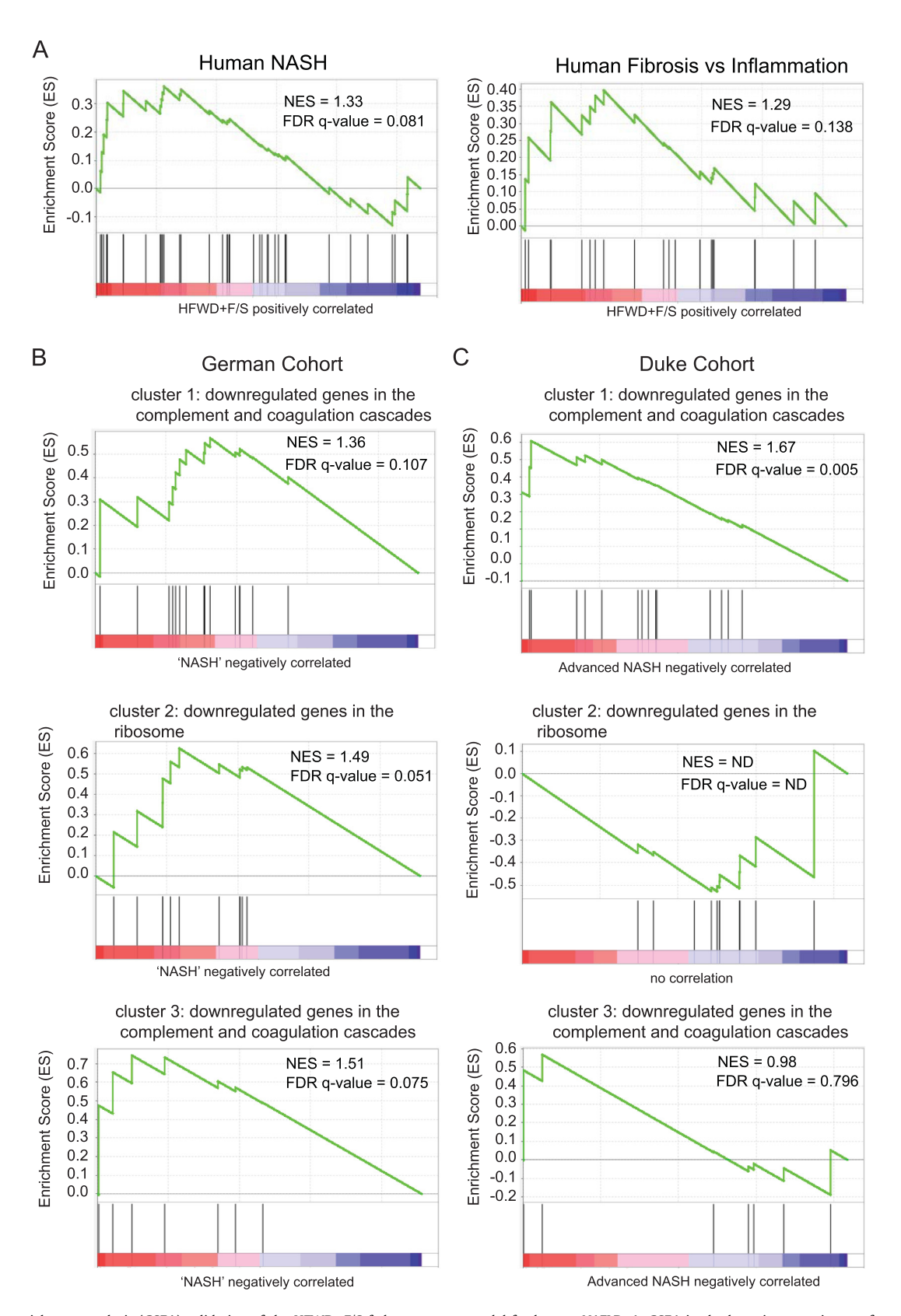


Fig. 4. Gene set enrichment analysis (GSEA) validation of the HFWD+F/S-fed mouse as a model for human NAFLD. A. GSEA in the hepatic transcriptome from HFWD+F/S-fed mice using a set of 90 hepatic genes significantly differentially expressed in human samples from NASH patients compared to control liver tissue (left panel) and a set of 38 genes differentially regulated between lobular inflammation and advanced fibrosis in human samples (right panel). Normalized enrichment score (NEW) and the FDE q-value are shown. B-C. Gene set enrichment in human NASH cohorts was performed using the upregulated and downregulated gene sets derived from the pathways identified in the gene clusters for HFWD+F/S from Fig. 2G. A. GSEA for our dataset against genes identified in patients exhibiting all stages of NAFLD in the Universitätsklinikum Dresden cohort (German Cohort, GSE48452). B. GSEA for our data set against genes identified in 72 patients classified as obese or overweight and exhibiting NAFLD with varying stages of fibrosis as identified in the Duke University cohort (Duke Cohort, GSE49541). GSEA was performed by comparing "Control vs NASH" (German Cohort) and "Mild vs Advanced" (Duke Cohort). Normalized enrichment score (NES) and the FDR q-value are shown.

to previous mouse studies and the human NAFLD/NASH condition was assessed using GSEA of our datasets against murine and human NASH gene sets and human NASH cohorts. We also examined the relevance of the complement and coagulation cascades biological process in the livers of HFWD+F/S-fed mice by focusing on the hepatic expression of genes for the ORM family of inflammatory proteins and the correlation between gene expression and NAFLD-related parameters.

Consistent with our prior findings [17,55,56], F/S consumption in HFWD-fed mice resulted in a large increase in body weight as well as normalized liver weight after 12 weeks. Histological scoring of stained liver tissue sections revealed that the HFWD+F/S group has the greatest steatosis, hypertrophy, and total NAFLD score, indicating that the combination of liquid fructose/sucrose and HFWD accelerates NAFLD. Consistent with these findings we observed enrichment of murine fibrosis and human NASH-related gene sets in the hepatic transcriptomic from HFWD+F/S-fed mice. Taken together these results confirm the validity of our model used to explore global changes in the hepatic transcriptome induced by fructose/sucrose water consumption in HFWD-fed mice.

We also observed fewer DEGs in HFWD vs. Chow compared to the HFWD+F/S vs. Chow, suggesting that liquid fructose/sucrose consumption uniquely reprograms the hepatic transcriptome. Indeed, a total of 688 DEGs were identified in the HFWD+F/S vs. Chow comparison, 314 of which were shared between the HFWD and HFWD+F/S groups, but 374 were uniquely observed in the HFWD+F/S group. These results provide compelling evidence that the combination of HFWD and liquid fructose/sucrose has a profound and distinct effect on gene expression in liver.

Our finding that genes in the complement and coagulation cascades pathway were differentially expressed is consistent with a recent report that alterations in complex complement and coagulation cascade regulation is observed to coincide with the development of inflammation and steatosis in the livers of NAFLD patients that also coincides with the development of inflammation in steatotic livers [57]. Complement and coagulation cascades pathway enrichment has also been observed in other murine NASH models including high-fat diet fed senescence-accelerated mouse prone 6 (SAMP6) mice [58] and long-term American lifestyleinduced obesity syndrome (ALIOS) diet-fed male mice [59]. It was proposed that the regulation of complement and coagulation cascade genes occurs prior to the development of advanced NASH in high-risk obese adults [57], which is consistent with our observations herein and validates the use of the HFWD+F/S mouse as a model for obese humans with mild NASH [16].

To further examine the regulation of complement and coagulation cascades in the livers from HFWD+F/S-fed mice, we focused on up-regulated expression of ORM. We observed a substantial increase in hepatic gene expression of ORM 1-3 in HFWD+F/Sfed mice. This data correlated with increased obesity, glucose intolerance, insulin resistance and a higher NAFLD score from our previous work using the HFWD+F/S mouse [17]. In humans, the serum concentration of ORM has been observed to be elevated in obese and diabetic patients and has been suggested to be a biomarker for obesity-induced metabolic disorders and inflammation [60-62]. In adipose tissue, overexpression of ORM has been shown to suppress pro-inflammatory gene expression and relieves hyperglycemia-induced insulin resistance, while the knockdown of ORM1 promotes both basal and TNF α -induced expression pro-inflammatory genes and disrupts insulin-stimulated glucose uptake. Hence, ORM is an integrator for inflammatory and metabolic signals that may protect from severe inflammation and metabolic dysfunction [63]. Indeed, we observed a significant elevation of hepatocyte gene expression of ORM isoforms in response to TNF α and FFAs together with hypoxia treatment in a dosedependent manner. Furthermore, we found positive correlations between the *ORM* (*ORM1-3*) gene expression and normalized liver to body weight and ALT while negative correlations between *ORM* (*ORM1-3*) gene expression and fibrosis were observed. Together, these results suggest that ORMs may have a similar protective effect in the liver. However, further studies are warranted to test the protective role of ORMs in the development of NASH.

A strength of our study is that murine and human NASH gene sets were found to be enriched in the hepatic transcriptomic data from HFWD+F/S-fed mice. Consistent with the mild NASH phenotype of high-fat Western diet with fructose/sucrose water consumption model of obesity [16,17], we did not observe significant enrichment of a human inflammation verses NASH gene set in the hepatic transcriptomic data from HFWD+F/S-fed mice. An additional strength of our study is that HFWD+F/S-linked network cluster genes in the complement and coagulation cascades pathway were found to be enriched in human NAFLD cohorts. A limitation of our study is that we only examined NAFLD parameters in male mice at a single time point which corresponds to an early stage in the development of NASH [59]. An additional limitation is that calories from the sugary drinking water may have contributed to our findings in the HFWD+F/S-fed mice. However, we have previously observed that total caloric intake and calories from the food in the HFWD-fed mice compared to the HFWD+F/S-fed mice is not significantly different after both 2-week and 12-weeks on the respective diets, and that only approximately 2.7% of the total calories in the HFWD+F/S-fed mice is from the sugar in the drinking water [17]. The lack of dietary assessment in the patient cohort used to examine the relevance of the hepatic HFWD+F/S network clusters is an additional limitation.

In summary, we demonstrate herein that the combination of a HFWD with F/S in the drinking water exacerbates HFWD-induced hepatic steatosis and NAFLD that is consistent with progression to NASH. More importantly, 12 weeks of HFWD+F/S feeding results in distinct reprogramming of the hepatic transcriptome with alterations in the most notable changes occurring in the complement and coagulation cascade gene pathway. The ORM family of inflammatory proteins may play a role in the mechanism of these unique alterations, however, this requires formal testing. Importantly, our results provide insight into the possible molecular basis by which the addition of fructose/sucrose water to a high-fat Western diet promotes the progression of NAFLD.

Data availability

The raw RNA seq data has been deposited in the NCBI Gene Expression Omnibus database: https://www.ncbi.nlm.nih.gov/geo/query/acc.cgi?token=uxexqkcgpzuhvwh&acc=GSE89296

Financial Support

This material is based upon work that is supported by the National Institute of Food and Agriculture, U.S. Department of Agriculture, Hatch/Multistate project Accession ALA044-1-18037 to MWG. We wish to acknowledge the support of the Haggard Family Annual Undergraduate Research Award in Nutrition and Dietetics to YL. Contributions from XW is supported by the USDA National Institute of Food and Agriculture, Hatch project 1018100 and a National Science Foundation EPSCoR RII Track-4 Research Fellowship (OIA1928770).

Conflict of Interest

The authors have no conflict of interest to declare.

Acknowledgments

We wish to thank the staff at the Biological Resources Facility for the care of the animals. We also wish to thank the HudsonAlpha Institute for Biotechnology Genomic Services Laboratory staff for performing the RNA sequencing.

Funding

This material is based upon work that is supported by the National Institute of Food and Agriculture, U.S. Department of Agriculture, Hatch/Multistate project Accession No. 1002087 to MWG. We wish to acknowledge the support of the Haggard Family Annual Undergraduate Research Award in Nutrition and Dietetics to YL. Contributions from XW is supported by the USDA National Institute of Food and Agriculture, Hatch project 1018100 and a National Science Foundation EPSCoR RII Track-4 Research Fellowship (OIA1928770).

Supplementary materials

Supplementary material associated with this article can be found, in the online version, at doi:10.1016/j.jnutbio.2022.109174.

CRediT authorship contribution statement

Yuwen Luo: Conceptualization, Writing – original draft, Methodology. Lauren N. Woodie: Investigation, Writing – original draft, Writing – review & editing, Visualization. Emily C. Graff: Investigation, Writing – review & editing. Jian Zhang: Investigation, Writing – review & editing. Savanah Fowler: Investigation. Xiaozhu Wang: Data curation, Investigation. Xu Wang: Data curation, Investigation, Writing – review & editing. Ann Marie O'Neill: Investigation. Michael W. Greene: Supervision, Investigation, Visualization, Writing – original draft, Methodology, Writing – review & editing.

References

- [1] Loomba R, Sanyal AJ. The global NAFLD epidemic. Nat Rev Dis Primers 2013;10:686–90.
- [2] Jung Y, Diehl AM. Non-alcoholic steatohepatitis pathogenesis: role of repair in regulating the disease progression. Dig Dis 2010;28:225–8.
- [3] Byrne CD, Targher G. NAFLD: a multisystem disease. J Hepatol 2015;62:S47-64.
- [4] Eslam M, Sanyal AJ, George J, Sanyal A, Neuschwander-Tetri B, Tiribelli C, et al. MAFLD: a consensus-driven proposed nomenclature for metabolic associated fatty liver disease. Gastroenterology 2020;158:1999–2014 e1.
- [5] Polyzos SA, Kang ES, Tsochatzis EA, Kechagias S, Ekstedt M, Xanthakos S, et al. Commentary: nonalcoholic or metabolic dysfunction-associated fatty liver disease? The epidemic of the 21st century in search of the most appropriate name. Metabolism 2020;113:154413.
- [6] Neuschwander-Tetri BA. Therapeutic landscape for NAFLD in 2020. Gastroenterology 2020;158:1984–98 e3.
- [7] Welsh JA, Sharma A, Abramson JL, Vaccarino V, Gillespie C, Vos MB. Caloric sweetener consumption and dyslipidemia among US adults. Jama 2010;303:1490-7.
- [8] Reedy J, Krebs-Smith SM. Dietary sources of energy, solid fats, and added sugars among children and adolescents in the United States. J Am Diet Assoc 2010;110:1477–84.
- [9] Vos MB, Lavine JE. Dietary fructose in nonalcoholic fatty liver disease. Hepatology 2013;57:2525-31.
- [10] Softic S, Stanhope KL, Boucher J, Divanovic S, Lanaspa MA, Johnson RJ, et al. Fructose and hepatic insulin resistance. Crit Rev Clin Lab Sci 2020;57:308–22.
- [11] Herman MA, Birnbaum MJ. Molecular aspects of fructose metabolism and metabolic disease. Cell Metab 2021;33:2329–54.
- [12] Helsley RN, Moreau F, Gupta MK, Radulescu A, DeBosch B, Softic S. Tissue-specific fructose metabolism in obesity and diabetes. Curr Diab Rep 2020;20:1–16.
- [13] Charlton M, Krishnan A, Viker K, Sanderson S, Cazanave S, McConico A, et al. Fast food diet mouse: novel small animal model of NASH with ballooning, progressive fibrosis, and high physiological fidelity to the human condition. Am J Physiol Gastrointest Liver Physiol 2011;301:G825–34.

- [14] Kohli R, Kirby M, Xanthakos SA, Softic S, Feldstein AE, Saxena V, et al. High-fructose, medium chain trans fat diet induces liver fibrosis and elevates plasma coenzyme Q9 in a novel murine model of obesity and nonalcoholic steatohepatitis. Hepatology 2010;52:934–44.
- [15] Tetri LH, Basaranoglu M, Brunt EM, Yerian LM, Neuschwander-Tetri BA. Severe NAFLD with hepatic necroinflammatory changes in mice fed trans fats and a high-fructose corn syrup equivalent. Am J Physiol Gastrointest Liver Physiol 2008:295:G987–95.
- [16] Machado MV, Michelotti GA, Xie G, Almeida Pereira T, Boursier J, Bohnic B, et al. Mouse models of diet-induced nonalcoholic steatohepatitis reproduce the heterogeneity of the human disease. PloS one 2015;10:e0127991.
- [17] Luo Y, Burrington CM, Graff EC, Zhang J, Judd RL, Suksaranjit P, et al. Metabolic phenotype and adipose and liver features in a high-fat Western diet-induced mouse model of obesity-linked NAFLD. Am J Physiol Endocrinol Metab 2016;310:E418–39.
- [18] Wang Z, Gerstein M, Snyder M. RNA-Seq: a revolutionary tool for transcriptomics. Nat Rev Genet 2009;10:57–63.
- [19] Nishikawa S, Sugimoto J, Okada M, Sakairi T, Takagi S. Gene expression in livers of BALB/C and C57BL/6J mice fed a high-fat diet. Toxicol Pathol 2012;40:71–82.
- [20] Oh HY, Shin SK, Heo HS, Ahn JS, Kwon EY, Park JH, et al. Time-dependent network analysis reveals molecular targets underlying the development of diet-induced obesity and non-alcoholic steatohepatitis. Genes & Nutr 2013;8:301–16.
- [21] Sreekumar R, Rosado B, Rasmussen D, Charlton M. Hepatic gene expression in histologically progressive nonalcoholic steatohepatitis. Hepatology 2003:38:244–51.
- [22] Younossi ZM, Baranova A, Ziegler K, Del Giacco L, Schlauch K, Born TL, et al. A genomic and proteomic study of the spectrum of nonalcoholic fatty liver disease. Hepatology 2005;42:665–74.
- [23] Liang W, Menke AL, Driessen A, Koek GH, Lindeman JH, Stoop R, et al. Establishment of a general NAFLD scoring system for rodent models and comparison to human liver pathology. PloS one 2014;9:e115922.
- [24] Greene MW, Burrington CM, Luo Y, Ruhoff MS, Lynch DT, Chaithongdi N. PKCdelta is activated in the liver of obese Zucker rats and mediates diet-induced whole body insulin resistance and hepatocyte cellular insulin resistance. J Nutr Biochem 2014;25:281–8.
- [25] Greene MW, Ruhoff MS, Burrington CM, Garofalo RS, Oreña SJ. TNFα activation of PKCδ, mediated by NFκB and ER stress, cross-talks with the insulin signaling cascade. Cell Signal 2010;22:274–84.
- [26] Hotamisligil G. Mechanisms of TNF-α-induced insulin resistance. Exp Clin Endocrinol diabetes 1999;107:119–25.
- [27] Lam TK, Yoshii H, Haber CA, Bogdanovic E, Lam L, Fantus IG, et al. Free fatty acid-induced hepatic insulin resistance: a potential role for protein kinase C-δ. Am J Physiol Endocrinol Metab 2002;283:E682–EE91.
- [28] Nakamura S, Takamura T, Matsuzawa-Nagata N, Takayama H, Misu H, Noda H, et al. Palmitate induces insulin resistance in H4IIEC3 hepatocytes through reactive oxygen species produced by mitochondria. J Biol Chem 2009:284:14809–18.
- [29] Lo KA, Labadorf A, Kennedy NJ, Han MS, Yap YS, Matthews B, et al. Analysis of in vitro insulin-resistance models and their physiological relevance to in vivo diet-induced adipose insulin resistance. Cell Rep 2013;5:259–70.
- [30] Gu CJ, Yi HH, Feng J, Zhang ZG, Zhou J, Zhou LN, et al. Intermittent hypoxia disrupts glucose homeostasis in liver cells in an insulin-dependent and independent manner. Cell Physiol Biochem 2018;47:1042–50.
- [31] Langmead B, Trapnell C, Pop M, Salzberg SL. Ultrafast and memory-efficient alignment of short DNA sequences to the human genome. Genome Biol 2009;10:1.
- [32] Trapnell C, Pachter L, Salzberg SL. TopHat: discovering splice junctions with RNA-Seq. Bioinformatics 2009;25:1105–11.
- [33] Li H, Handsaker B, Wysoker A, Fennell T, Ruan J, Homer N, et al. The sequence alignment/map format and SAMtools. Bioinformatics 2009;25:2078–9.
- [34] Robinson MD, Oshlack A. A scaling normalization method for differential expression analysis of RNA-seq data. Genome Biol 2010;11:1.
- [35] Benjamini Y, Hochberg Y. Controlling the false discovery rate: a practical and powerful approach to multiple testing. J R Stat Soc Series B (Methodological) 1995;57(1):289–300.
- [36] Huang DW, Sherman BT, Lempicki RA. Bioinformatics enrichment tools: paths toward the comprehensive functional analysis of large gene lists. Nucleic Acids Res 2008;37:1–13.
- [37] Huang DW, Sherman BT, Lempicki RA. Systematic and integrative analysis of large gene lists using DAVID bioinformatics resources. Nat Protoc 2009;4:44.
- [38] Kanehisa M, Goto S. KEGG: kyoto encyclopedia of genes and genomes. Nucleic Acids Res 2000;28:27–30.
- [39] Franceschini A, Szklarczyk D, Frankild S, Kuhn M, Simonovic M, Roth A, et al. STRING v9. 1: protein-protein interaction networks, with increased coverage and integration. Nucleic Acids Res 2012;41:D808–DD15.
- [40] Smoot ME, Ono K, Ruscheinski J, Wang P-L, Ideker T. Cytoscape 2.8: new features for data integration and network visualization. Bioinformatics 2010;27:431–2.
- [41] Bader GD, Hogue CW. An automated method for finding molecular complexes in large protein interaction networks. BMC Bioinformatics 2003;4:2.
- [42] Subramanian A, Tamayo P, Mootha VK, Mukherjee S, Ebert BL, Gillette MA, et al. Gene set enrichment analysis: a knowledge-based approach for interpreting genome-wide expression profiles. Proc Natl Acad Sci U S A 2005;102:15545–50.

- [43] Mesirov JP, Tamayo P. Gene Set Enrichment Analysis (GSEA) User Guide. Boston. Massachusetts: Broad Institute: 2020.
- [44] van Koppen A, Verschuren L, van den Hoek AM, Verheij J, Morrison MC, Li K, et al. Uncovering a predictive molecular signature for the onset of nash-related fibrosis in a translational NASH mouse model. Cell Mol Gastroenterol Hepatol 2017;5:83–98 e10.
- [45] Teufel A, Itzel T, Erhart W, Brosch M, Wang XY, Kim YO, et al. Comparison of gene expression patterns between mouse models of nonalcoholic fatty liver disease and liver tissues from patients. Gastroenterology 2016;151:513–25 e0.
- [46] Gerhard GS, Legendre C, Still CD, Chu X, Petrick A, DiStefano JK. Transcriptomic profiling of obesity-related nonalcoholic steatohepatitis reveals a core set of fibrosis-specific genes. J Endocr Soc 2018;2:710–26.
- [47] Davis S, Meltzer PS. GEOquery: a bridge between the Gene Expression Omnibus (GEO) and BioConductor. Bioinformatics 2007;23:1846–7.
- [48] Ahrens M, Ammerpohl O, von Schönfels W, Kolarova J, Bens S, Itzel T, et al. DNA methylation analysis in nonalcoholic fatty liver disease suggests distinct disease-specific and remodeling signatures after bariatric surgery. Cell Metab 2013:18:296–302.
- [49] Kleiner DE, Brunt EM, Van Natta M, Behling C, Contos MJ, Cummings OW, et al. Design and validation of a histological scoring system for nonalcoholic fatty liver disease. Hepatology 2005;41:1313–21.
- [50] Livak KJ, Schmittgen TD. Analysis of relative gene expression data using real-time quantitative PCR and the 2(-Delta Delta C(T)) Method. Methods 2001;25:402–8.
- [51] Tiniakos DG, Vos MB, Brunt EM. Nonalcoholic fatty liver disease: pathology and pathogenesis. Annu Rev Pathol 2010;5:145–71.
- [52] Powell AE, Wang Y, Li Y, Poulin EJ, Means AL, Washington MK, et al. The pan-ErbB negative regulator Lrig1 is an intestinal stem cell marker that functions as a tumor suppressor. Cell 2012;149:146-58.
- [53] Fournier T, Medjoubi NN, Porquet D. Alpha-1-acid glycoprotein. Biochimi et Biophys Acta 2000;1482:157–71.
- [54] Hochepied T, Berger FG, Baumann H, Libert C. Alpha(1)-acid glycoprotein: an acute phase protein with inflammatory and immunomodulating properties. Cytokine & Growth Factor Reviews 2003;14:25–34.

- [55] Woodie LN, Johnson RM, Ahmed B, Fowler S, Haynes W, Carmona B, et al. Western diet-induced obesity disrupts the diurnal rhythmicity of hippocampal core clock gene expression in a mouse model. Brain Behav Immun 2020;88:815-25
- [56] Woodie LN, Luo Y, Wayne MJ, Graff EC, Ahmed B, O'Neill AM, et al. Restricted feeding for 9 h in the active period partially abrogates the detrimental metabolic effects of a Western diet with liquid sugar consumption in mice. Metabolism 2018:82:1–13.
- [57] Subudhi S, Drescher HK, Dichtel LE, Bartsch LM, Chung RT, Hutter MM, et al. Distinct hepatic gene-expression patterns of NAFLD in patients with obesity. Hepatol Commun.n/a.
- [58] Almanza D, Gharaee-Kermani M, Zhilin-Roth A, Rodriguez-Nieves JA, Colaneri C, Riley T, et al. Nonalcoholic fatty liver disease demonstrates a pre-fibrotic and premalignant molecular signature. Dig Dis Sci 2019;64:1257–69.
- [59] Harris SE, Poolman TM, Arvaniti A, Cox RD, Gathercole LL, Tomlinson JW. The American lifestyle-induced obesity syndrome diet in male and female rodents recapitulates the clinical and transcriptomic features of nonalcoholic fatty liver disease and nonalcoholic steatohepatitis. Am J Physiol Gastrointest Liver Physio 2020;319:G345–Gg60.
- [60] Range H, Poitou C, Boillot A, Ciangura C, Katsahian S, Lacorte JM, et al. Oroso-mucoid, a new biomarker in the association between obesity and periodontitis. PloS one 2013;8:e57645.
- [61] Alfadda AA, Fatma S, Chishti MA, Al-Naami MY, Elawad R, Mendoza CD, et al. Orosomucoid serum concentrations and fat depot-specific mRNA and protein expression in humans. Mol Cells 2012;33:35–41.
- [62] Dandona P, Aljada A, Bandyopadhyay A. Inflammation: the link between insulin resistance, obesity and diabetes. Trends Immunol 2004;25:4–7.
- [63] Lee YS, Choi JW, Hwang I, Lee JW, Lee JH, Kim AY, et al. Adipocytokine orosomucoid integrates inflammatory and metabolic signals to preserve energy homeostasis by resolving immoderate inflammation. J Biol Chem 2010;285:22174–85.